

CONTROL OF MEMS ON THE EDGE OF INSTABILITY

C.B.Burgner, W.S.Snyders, and K.L.Turner

University of California, Santa Barbara, California, USA

ABSTRACT

This paper investigates a new method for tracking parameters at which dynamic bifurcations occur in MEMS based on state statistics of a resonator. Experimental results show that observed changes in phase and amplitude precede a sub-critical pitchfork bifurcation. Feedback control, based on the statistics of the phase, is then employed to stabilize a device on the edge of instability. Sensitivity to changes in device parameters is explored and initial results show high sensitivity is obtained for low vibration amplitudes. Furthermore, experimental results on the same device using an older method of bifurcation sensing show acquisition rate improvement by over three orders of magnitude with the new method.

KEYWORDS

Bifurcation, mass sensing, feedback control

INTRODUCTION

The small size of MEMS and their integration with electronics provide fast, precise and highly sensitive measurement of changes in their parameters which has mass sensing applications [1-5]. Linear mass sensing is based on the correlation between shifts in device resonant frequency and acquired mass. As linear mass sensing has become the standard for MEMS mass sensing, fundamental thermo-mechanical noise limitations in both linear and parametrically amplified resonators have been derived [6,7]. Although large amplitude oscillations are favorable to increase the signal to noise ratio, it has been established that no improvement is gained using parametric amplification over sensors operated in the linear regime [6].

Utilizing bifurcations in MEMS resonators has been introduced as a different approach to mass sensing. Bifurcations are purely nonlinear phenomena that exhibit qualitative changes in dynamics where fixed points can be created or destroyed, or change in stability [8]. Bifurcation mass sensing is founded on the correlation between shifts in bifurcation points and acquired mass. Previous bifurcation sensing techniques require parametric excitation parameters to be swept towards a sub-critical pitchfork bifurcation point until a "jump event" in amplitude is observed and its location is noted [9-11]. Limitations on mass sensitivity resolution of bifurcation sweep sensing methods are also due to thermo-mechanical noise which blurs the location of the jump event. The role excitation parameter sweep rate and resonator noise strength has in blurring the distribution of jump events has been shown over a wide range of sweep rate to noise strength ratios [11].

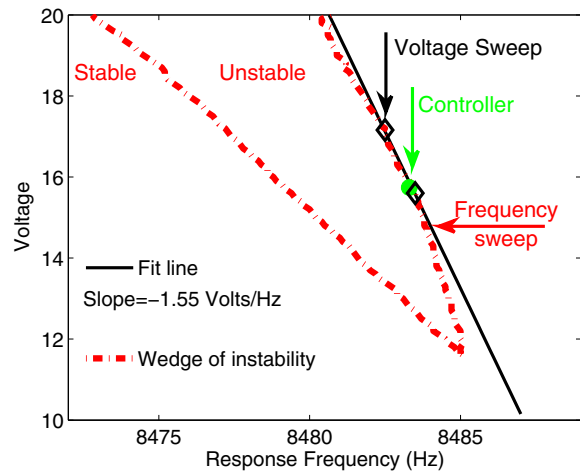


Figure 1: Dashed line represents the "wedge of instability," inside of which zero vibration amplitude goes unstable. The dashed line is found experimentally by sweeping the frequency at actuation voltages between 11 and 20 Volts. For two given frequencies, represented by diamonds, the voltage is swept using bifurcation based approach. Solid black line is fit in proximity to the controller set point using the voltage and frequency sweep distributions.

Because the vibration amplitude of the jump event is pushed into the nonlinear regime, bifurcation sensing has been shown to perform well in circumstances where measurement noise is the dominant source of parameter uncertainty [10]. Time is required after each jump event to reset the system back to appropriate initial conditions and hysteresis must be avoided to allow consecutive parameter sweeps to take place. The reset time greatly impedes the acquisition rate making it vulnerable to slow changes in environmental conditions and excludes it from dynamic parameter sensing applications.

In this paper we take an entirely different approach than either linear sensing or previous bifurcation sweeping methods. By controlling the excitation parameters, we stabilize a resonator near a bifurcation point based on statistics of its squeezed state which act as a precursor to the jump event. The required control action, proportional to statistics of the state, is then indicative of the device's proximity to the bifurcation point. Since no jump event takes place, long settling times and hysteresis are avoided. This enables acquisition rate improvement over previous bifurcation sweeping methods. Another advantage of this method is the restrained vibration amplitudes at which measurements take place. As opposed to previous bifurcation and linear sensing methods, this technique keeps the amplitude of vibration small while still allowing for sensitive measurements. We show an improved acquisition rate over previous bifurcation sweeping methods and demonstrate low amplitude vibration is maintained

through experimental results for a controller based on observing the squeezed state of a parametrically excited resonator.

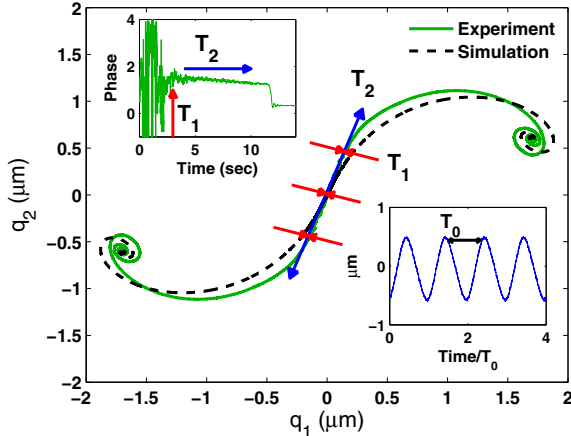


Figure 2: Experimental and simulated escape event. Squeezing onto and motion along the slow manifold occur on time scales T_1 and T_2 respectively, illustrated by their associated arrows. Two fixed points exist 180° apart. The fastest time scale is the period of oscillation, $T_0 = 0.11\text{mSec}$

CONTROLLER OPERATION

The device used as a prototype for noise squeezing control is a parametrically excited gyroscope that has been fully characterized including nonlinear parameters encountered during a sub-critical pitchfork bifurcation [12]. Although the gyroscope is a two degree of freedom system, the drive and sense mode are mismatched by over 7% which permits each mode to be studied separately. The drive mode has a resonant frequency near 8448Hz and a quality factor in vacuum near 3000. Drive mode actuation is applied through non-interdigitated comb drives resulting in a forcing strength dependent on both the resonator position and the applied voltage. The single degree of freedom motion in the drive mode is governed by a nonlinear Mathieu equation (1) where z is the position of the resonator, the overdot represents time derivative, Γ is the scaled damping coefficient, ω_0 is the resonant frequency, δ is the forcing applied at approximately twice the resonant frequency, γ is the cubic nonlinearity and ξ is white noise with strength D . Equation (1) has been studied extensively in the context of MEMS [9-16].

$$\ddot{z} + 2\Gamma\dot{z} + \omega_0^2(1 + \delta + \delta\cos 2\omega t)z + \gamma z^3 = \xi(t) \quad (1)$$

$$\langle \xi(t) \rangle = 0 \quad \langle \xi(t)\xi(t') \rangle = 2D\delta(t - t') \quad (2)$$

In this work, we show experimental evidence of two features: the “wedge of instability” region or transition curve and the existence of a slow manifold. Both features are predicted for device behavior governed by equation (1) and are essential for controller operation. First, Fig. 1 shows the experimental boundary for the “wedge of instability.” The wedge location, dashed line in Fig. 1, is obtained by sweeping the excitation frequency near twice

the resonant frequency at voltages between 12 and 20 Volts. For excitation voltages and frequencies inside the wedge, the zero solution of equation (1) goes unstable. The loss of stability is due to either a sub-critical or supercritical pitchfork bifurcation which, for our device, occurs along the right or left side of the wedge respectively. It should be noted the device response occurs at half the excitation frequency.

To investigate the existence of the slow manifold, a change of coordinates (q_1, q_2) into a frame rotating at the response frequency is used. In the rotating frame, the amplitude of vibration is represented by the sum of squares q_1 and q_2 . The phase of oscillation with respect to the excitation frequency is the two argument tangent of q_1 and q_2 . Figure 2 shows the escape trajectory in the rotating frame during a sub-critical pitchfork bifurcation. We observe the zero state loses stability and moves along an existent slow manifold to a stable fixed point of large vibration amplitude. Also note the symmetric two solutions 180° apart. Experimental investigation of the slow manifold verifies a separation time scales, illustrated by their arrows in Fig. 2. The fastest time scale is the natural period of oscillation T_0 , shown in the lower inset of Fig. 2. The next fastest time scale, T_1 is the collapse onto the slow manifold, inversely proportional to the damping. The slowest time scale is the motion along the slow manifold, T_2 . The collapse onto and then motion along the slow manifold are shown in the upper inset of Fig. 2. Notice the motion along the slow manifold, $T_2 \approx 8\text{Sec}$, is much slower than the natural period of oscillation $T_0 = 0.11\text{mSec}$.

The sub-critical pitchfork bifurcation encountered at excitation parameters defined by the wedge and the subsequent collapse onto the slow manifold are the two phenomena used in controller operation. Near the bifurcation point, the state of the device is squeezed onto the slow manifold, greatly reducing the variance of the phase, shown in the upper inset of Fig. 2. By using the variance of the phase as a precursor to bifurcation, the controller exploits the separation of time scales to adjust the excitation parameters such that the squeezed state is maintained but the jump event is avoided.

EXPERIMENT

The experimental setup is shown in Fig. 3. A function generator supplies the excitation voltage at a frequency near twice the resonant frequency. The laser vibrometer is used to measure the device velocity. The velocity signal is sent to a phase lock amplifier, PLA, which transforms the signal into the rotating frame at half the drive frequency. The PLA provides amplitude and phase information to the controller. The controller is implemented on a National Instruments CompactRIO platform which contains a field programmable gate array (FPGA).

The replacement of fast dedicated analog circuits with digital control is made possible by the separation of time scales. The digital controller operation is shown

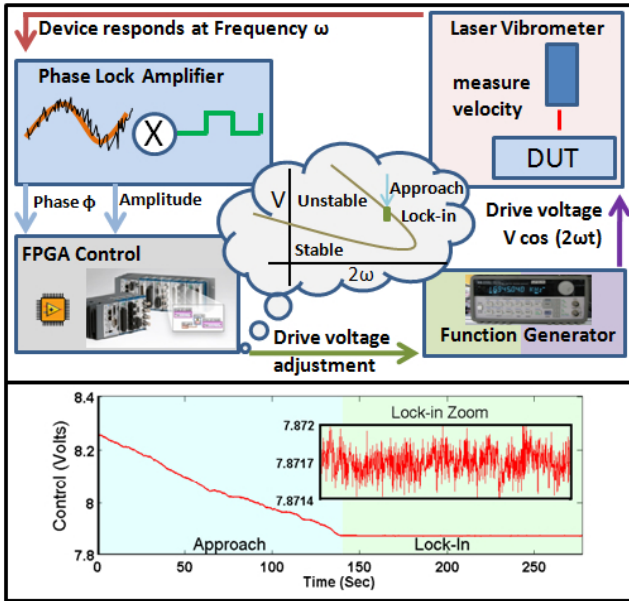


Figure 3: Function generator provides a drive signal near twice the resonant frequency while simultaneously a trigger to the phase lock amplifier (PLA) at response frequency. Control is carried out on an FPGA which uses statistics of amplitude and phase from the PLA to modify drive amplitude and maintain proximity to the bifurcation point. Experimental approach and lock-in stage of the controller is shown below.

schematically in the idea of cloud Fig. 3. First, the controller sweeps voltage downward towards the wedge during the approach stage, experimental control action is shown in the lower section of Fig. 3. During approach, the phase is randomly distributed between $\pm\pi$ resulting in a variance of 2.42. Suddenly, in close proximity to the critical point and on the time scale of T_1 , the phase collapses onto the attendant manifold reducing the phase variance to 0.02. The digital controller switches gains in the lock-in stage and maintains the small variance of the squeezed state but stays far enough away from the critical point to avoid the jump event to either stable fixed point shown in Fig. 2.

Amplitude and phase of the device is shown during the approach and lock-in stage of the controller operation in Fig. 4. Notice that although the amplitude stays small, the phase variance is noticeably squeezed by two orders of magnitude making it a viable metric for control.

DISCUSSION

To increase sensitivity, linear mass sensing strategies have pushed the amplitude of oscillation to its limits of linearity and control beyond the critical point has also been studied [17]. Bifurcation sweeping produces amplitudes governed by device nonlinearity and consequently larger signal to noise ratios can be obtained [10]. In Fig. 4 we show the amplitude is kept very small in comparison to the bifurcation sweeping or linear methods applied to this device.

Displacement at the forcing frequency is present due to the direct forcing component from the comb drives. The parasitic displacement is shown in Fig. 5. Note that

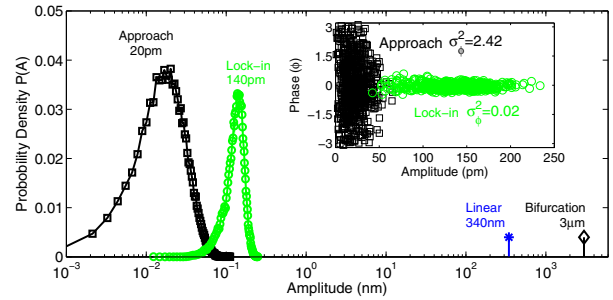


Figure 4: Distribution of vibration amplitude during “approach” and at controller “lock-in.” For vibration amplitude comparison, typical amplitudes required of linear sensing and those observed during bifurcation sweeping methods are shown for this device.

the displacement stays constant throughout controller operation and is appreciable to the displacement signal of interest at the response frequency during both the approach and lock-in stage of control. The parasitic displacement is negligible in comparison to vibration amplitudes achieved during linear or bifurcation sweeping sensing methods. Noise squeezing control, which utilizes low vibration amplitude, not only reduces fatigue, but may also provide new capability for applications where large vibration amplitudes hinder measurements.

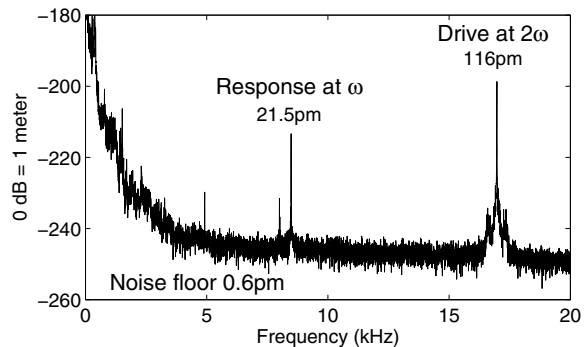


Figure 5: Displacement amplitude is shown for a wide band of frequencies. The response frequency occurs at half the drive frequency and at amplitude of five times less during the approach stage of the controller.

The sensitivity and acquisition rate of the noise squeezing controller are compared with the previous bifurcation sweeping method in Fig. 6. In Fig. 6 (A), the normalized error obtained by sweeping the frequency using the old bifurcation method is compared with the normalized error in voltage uncertainty from the noise squeezing controller. Both methods achieve a normalized excitation parameter uncertainty of width $\pm 5 \times 10^{-5}$. In Fig. 6 (B), the voltage distribution obtained by sweeping the voltage using the old bifurcation method is compared with the voltage distribution from the noise squeezing controller. The noise squeezing controller provides a voltage distribution that is over one hundred times narrower than voltage distribution obtained using the old bifurcation sweeping [11].

The acquisition rate for both bifurcation voltage and frequency sweeping methods are nearly equal measuring

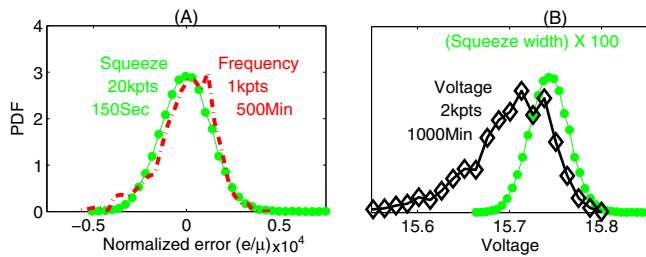


Figure 6: Controller voltage distribution (circles) is compared against experimental bifurcation sweeping of the frequency (A) and the voltage (B).

approximately 2 escape events per minute. For both frequency and voltage parameter sweeps, the upper limit of acquisition rate was achieved. Their acquisition rate similarity was not designed into the experiment but is a consequence of the maximum allowable acquisition rate dictated by requirements of initial conditions. Notice in Fig. 6 (A) that for the same normalized error in parameter uncertainty, indicative of minimum mass resolution, noise squeezing control outperforms the old method's acquisition rate by over three orders of magnitude.

Using the slope of the fit line in Fig. 1, the minimum frequency resolution is determined to be near 0.2mHz. It has been shown that the transition curve can be designed in the fabrication process and is also tunable [16]. The noise squeezing mass sensitivity may be further enhanced by designing the transition curve to have points of very steep slope and operating the controller near one of these points.

CONCLUSION

The sensitivity and acquisition rate is investigated for a new sensing method based on the squeezed state of a resonator near critical points. Experimental verification of the transition curve, the separation of time scales and noise squeezing, all essential to controller operation, are shown. Noise squeezing control acquisition rate is found to be over three orders of magnitude better than previous bifurcation sweeping methods and high sensitivity is shown for low amplitude vibrations.

REFERENCES

[1] Rongrui He, X. L. Feng, M. L. Roukes, and Peidong Yang. "Selftransducing silicon nanowire electromechanical systems at room temperature." *Nano Letters*, 8:1756–1761, 2007.

[2] K. L. Ekinici, X. M. H. Huang, and M. L. Roukes. "Ultrasensitive nanoelectromechanical mass detection." *Applied Physics Letters*, 84(22):4469, 2004.

[3] B. Ilic, H. G. Craighead, S. Krylov, W. Senaratne, C. Ober, and P. Neuzil. "Attogram detection using nanomechanical resonators." *Journal of Applied Physics*, 2004.S.

[4] T.P. Burg, M. Godin, S.M. Knudsen, W. Shen, G. Carlson, J.S. Foster, K. Babcock, and S.R. Manalis. "Weighing of biomolecules, single cells, and single

nanoparticles in fluid." *Nature*, 446:1066–1069, 2007.

[5] Nickolay V. Lavrik and Panos G. Datskos. "Femtogram mass detection using photothermally actuated nanomechanical resonators." *Applied Physics Letters*, 82(16):2697, 2003.

[6] Andrew N. Cleland. Thermomechanical noise limits on parametric sensing with nanomechanical resonators. *New Journal of Physics*, 7:235, 2005.

[7] K. Ekinici, Y. Yang, and M. Roukes. "Ultimate limits to inertial mass sensing based upon nanoelectromechanical systems." *Journal of Applied Physics*, 95:2682–2689, 2004.

[8] S. Strogatz, "Nonlinear Dynamics and Chaos", Westview Press, 2000.

[9] Michael V. Requa and K.L. Turner. Precise frequency estimation in a microelectromechanical parametric resonator. *Applied Physics Letters*, 90:173508–173508–3, 2007.

[10] Zi Yie, Mark A Zielke, Christopher B Burgner, and Kimberly L Turner. Comparison of parametric and linear mass detection in the presence of detection noise. *Journal of Micromechanics and Microengineering*, 21(2):025027, 2011.

[11] Chris Burgner, Nick Miller, Steve Shaw, and Kimberly Turner. Parameter sweep strategies for sensing using bifurcations in mems. *Solid-State Sensor, Actuator, and Microsystems Workshop, Hilton Head Workshop*, SC, June 2010.

[12] L. A. Oropeza-Ramos, C.B. Burgner, and K. L. Turner. "Robust micro-rate sensor actuated by parametric resonance." *Sensors and Actuators A: Physical*, 152:80–87, 2009.

[13] Kimberly. Turner, Scott. Miller, Peter. Hartwell, Noel. MacDonald, Steven. Strogatz, and Scott. Adams. "Five parametric resonances in a microelectromechanical system." *Nature*, 396:148–152, 1998.

[14] H. B. Chan, M. I. Dykman, and C. Stambaugh. "Switching-path distribution in multidimensional systems." *Phys. Rev. E*, 78(5):051109, Nov 2008.

[15] M.I. Dykman, C.M. Maloney, V.N. Smelyanskiy, and M. Silverstein. "Fluctuational phase-flip transitions in parametrically driven oscillators." *Physic Review E*, 57:5202–5212, 1998.

[16] B. DeMartini, J. Rhoads, K. Turner, S. Shaw, and J. Moehlis. Linear and nonlinear tuning of parametrically excited mems oscillators. *Journal of Microelectromechanical Systems*, 16:310–318, 2007.

[17] H K Lee, J C Salvia, S Yoneoka, G Bahl, Y Q Qu, R Melamud, S Chandorkar, M A Hopcroft, B Kim, and T W Kenny. Stable oscillation of mems resonators beyond the critical bifurcation point. Pages 70–73, *Solid-State Sensor, Actuator, and Microsystems Workshop, Hilton Head Workshop*, SC, June 2010.

CONTACT

* C.B. Burgner, cburgner@enr.ucsb.edu